RESEARCH PAPER

Structural, Magnetic and Photocatalytic Properties of $BiFeO_3$ Nanoparticles

Seyyed Morteza Masoudpanah * *and Seyed Mohammad Mirkazemi*

School of Metallurgy and Materials Engineering, Iran University of Science and Technology (IUST), Tehran, Iran

ARTICLE INFO

Article History:
Received 03 April 2017
Accepted 07 June 2017
Published 01 July 2017

Keywords:
$BiFeO_3$
Optical band gap
Photodegradation
Thermal decomposition

ABSTRACT

Single phase $BiFeO_3$ nanoparticles as a visible light photocatalyst were successfully synthesized by thermal decomposition of the glyoxylate precursor. The glyoxylate precursors were formed by the redox reaction between ethylene glycol and nitrate ions. The phase evolution, structure and optical properties of $BiFeO_3$ nanoparticles were characterized by X-ray diffraction, electron microscopy and UV–Vis spectroscopy methods. The $BiFeO_3$ nanoparticles showed the quasi spherical shape. The $BiFeO_3$ nanoparticles synthesized at 500 °C showed the weak ferromagnetism behavior, due to the size confinement effect, in spite of the antiferromagnetic behavior of the $BiFeO_3$ nanoparticles synthesized at 600 °C. The $BiFeO_3$ nanoparticles exhibited strong absorption in the visible region with the optical band gap calculated from Tauc's plot. The optical band gap decreased from 2.10 to 2.08 eV by the increasing of thermal decomposition temperature. Moreover, the $BiFeO_3$ nanoparticles were used for the degradation of methylene blue as a typical dye pollutant under direct sunlight irradiation.

How to cite this article
Masoudpanah S. M, Mirkazemi S. M. Structural, Magnetic and Photocatalytic Properties of $BiFeO_3$ Nanoparticles. J Nanostruct, 2017; 7(3):183-188. DOI: 10.22052/jns.2017.03.003

INTRODUCTION

TiO_2-based photocatalysts have been applied widely to degrade the organic pollutants for the remediation of hazardous wastes, contaminated groundwater and the control of toxic air contaminants [1]. However, the optical band gap of TiO_2 (3.0-3.2 eV for anatase) is so wide that it can only absorb ultraviolet (UV) light, which is only 5% in the sun source [2]. Hence, another class of oxides such as ferrites with the narrow optical band gap in the visible light region has gained much interest in recent years as potential visible catalysts for industrial processes. Among ferrites, bismuth ferrite with a rhombohedrally distorted perovskite structure is a new important visible light photocatalyst for the degradation of organic pollutants due to its narrow optical band gap energy (2.2 eV) and excellent chemical stability [3-5]. Furthermore, it is famous as a well-known multiferroic compound that demonstrates the coexistence of ferroelectric and antiferromagnetic order above room temperature. However, the BFO nanoparticles exhibit a weak ferrimagnetic order at room temperature which is quite different from the G-type antiferromagnetic behavior in the bulk. Moreover, the used magnetic BFO nanoparticles are easy to collect, which make them become one of the most promising photocatalysts in the field of industrial photodegradation of organic pollutants [6].

BFO nanoparticles have been synthesized by variety of low temperature chemical methods

* *Corresponding Author Email: masoodpanah@iust.ac.ir*

such as hydrothermal [7], coprecipitation [8], sol–gel [9], sonochemical and microemulsion methods [10]. Thermal decomposition of heteronuclear complexes is one of the simplest techniques for preparing nanosized perovskite-type oxides with relatively lower thermal decomposition temperatures, smaller particle size and higher homogeneity as compared to the conventional synthesis methods [11]. The heteronuclear complexes can be synthesized by the glyoxylate precursor method in which the carboxylate ions for chelating were formed by the redox reaction between polyols and nitrate ions at low temperatures (~100-130 °C). The carboxylate complexes were then thermally decomposed for forming simple or mixed oxides [11].

In this work, the structural, magnetic and photocatalytic properties of BFO nanoparticles synthesized by thermal decomposition of glyoxylate precursor were studied.

MATERIALS AND METHODS

The analytical grade $Fe(NO_3)_3.9H_2O$, $Bi(NO_3)_2.5H_2O$, ethylene glycol ($OH(CH_2)_2OH$) and nitric acid (68 wt.%) were provided from Merk Company. The heteronuclear complex (precursor) was prepared by dissolving 16 mmol of $Fe(NO_3)_3.9H_2O$ in 100 mmol ethylene glycol and then added into 15 mL of 3 mol/L nitric acid solution containing 16 mmol $Bi(NO_3)_3.5H_2O$ under magnetic stirring at 70 °C. The molar ratio of ethylene glycol:NO^-_3 was 2.5:1. With increasing the temperature up to 100 °C, the redox reaction between the NO^-_3 anions and the OH groups of the diol was initiated with the evolving of brown nitrogen oxides (NO_x). Finally, the dried precursor was decomposed at 500 and 600 °C for 2 h in air to obtain the BFO nanoparticles.

The phase evolution was investigated by X'pert Pro prefix X-ray diffractometer using monochromatic CuKα radiation. The Raman spectral analysis (Witech Alpha 300R, Nd:YAG laser source: λ = 532 nm and 0.7 mW power, and range: 100–600 cm^{-1}) was performed on the powder samples. The morphology and microstructure of the particles were observed by Philips CM200 transmission electron microscope (TEM) at 150 kV. A vibrating sample magnetometer (Meghnatis Daghigh Kavir Kashan Co., Iran) with maximum field of 10 kOe was employed to measure the magnetic properties of the samples at room temperature. The optical absorption spectrum was recorded on an Avaspec 2048 TEC UV–Vis spectrophotometer in the wavelength range of 300–800 nm.

Photocatalytic activity of the prepared BFO nanoparticles was evaluated by the degradation of methylene blue (MB) in aqueous solution under direct solar irradiation. In each experiment, 0.1 g of photocatalyst was added into 100 ml methylene blue solution with a concentration of 10 mg/l. Furthermore, the pH of solution was adjusted to 2 by adding HCl. The suspension was magnetically stirred in the dark for 60 min to establish the adsorption/desorption equilibrium, then the solution was irradiated using visible radiation. The change in the concentration of each degraded solution was monitored on UV–Vis–NIR spectrophotometer Raylight UV-1600.

RESULTS AND DISCUSSION

XRD patterns of the precursor decomposed at 500 °C and 600 °C are shown in Fig. 1. At 500 °C, the sample showed a mixture of $BiFeO_3$ and $Bi_{25}FeO_{39}$ phases. However, the minor impurity $Bi_{25}FeO_{39}$ phase disappeared with increasing the temperature up to 600 °C in which the single phase $BiFeO_3$ was formed. The peaks were also indexed as (012), (104), (110), (202), (024), etc. which are characteristics of pure single phase perovskite-type $BiFeO_3$ (JCPDS card no. 01-071-2494). The formation of the single phase $BiFeO_3$ at low temperature is due to the formation of a homogenous polyester precursor through the double bridge chelating of Fe^{3+} and Bi^{3+} cations with glyoxylate ligands [12]. Fig. 2 shows the Rietveld refinement results of the single phase $BiFeO_3$ nanoparticles synthesized at 600 °C. The refined lattice parameter was obtained as a = 5.575(3) Å and c = 13.871(5) Å which matches very well with the values reported in the literature (a = 5.590 Å and c = 13.869 Å) [13].

Fig. 3 shows the Raman spectrum of BFO nanoparticles synthesized at 600 °C. According to group theory, the rhombohedral BFO has 18 optical phonon modes: Γ=4A1+5A2+9E [14]. The A1 and E modes are Raman and infrared active, while the A2 modes are nonactive. The three peaks at 142, 168 and 216 cm^{-1} are assigned as A1 modes, and the peaks at 249, 268, 326, 428 and 520 cm^{-1} are denoted as E modes. Bands at low Raman shift is due to the Bi-O bonds, while the internal vibration of FeO6 units results in the bands at high Raman shift. The purity of BFO nanoparticles can be confirmed by the absence

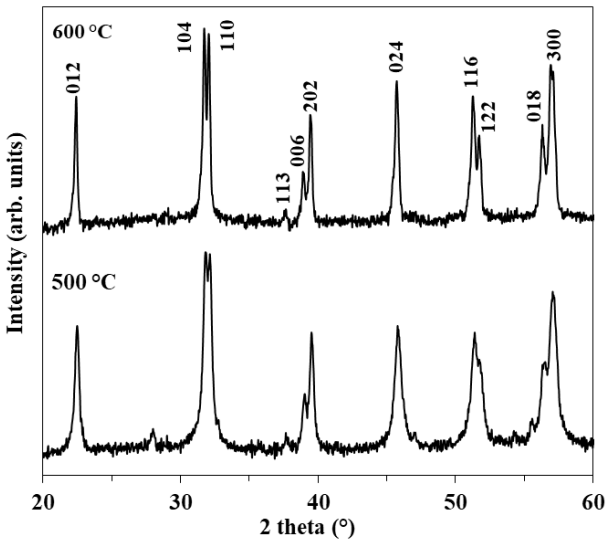

Fig. 1. XRD patterns of the precursor decomposed at 500 °C and 600 °C (white square indicates $Bi_{25}FeO_{39}$ and the other peaks are for $BiFeO_3$).

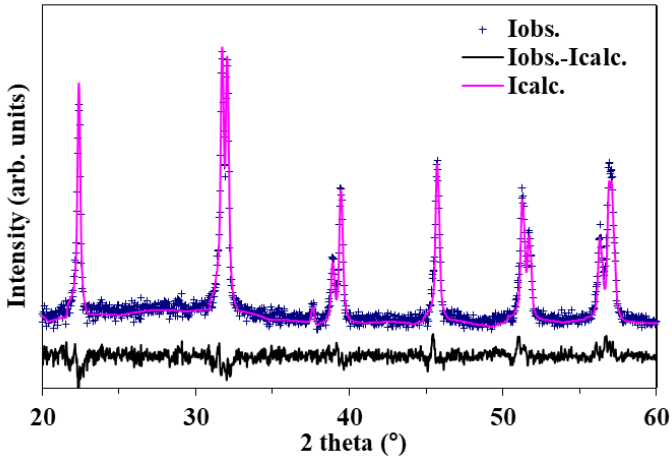

Fig. 2. XRD pattern and Rietveld refinement result of $BiFeO_3$ nanoparticles synthesized at 600 °C (The fitting indices of Rp, Rwp, and χ 2 are 12.7 %, 15.76 %, and 3.07, respectively).

of Raman modes corresponded to the impurity phases. Furthermore, the broadening of the high frequency modes on account of the small size of BFO nanoparticles eliminates the low frequency modes.

TEM images of BFO nanoparticles synthesized at 500 °C and 600 °C are shown in Fig. 4. The particles have quasi spherical shapes. The average particle size increases from 45 to 130 nm with increasing of the thermal decomposition temperature. Furthermore, the BFO nanoparticles synthesized at 500 °C exhibited a relatively narrow particle size distribution which becomes wider at 600 °C.

Fig. 5 shows the room temperature magnetization curves of the BiFeO3 nanoparticles synthesized at 500 and 600 °C. In bulk BFO, the presence of spiral spin arrangement of wavelength 62 nm is responsible for the suppression of magnetization [15]. From the TEM micrographs, it is observed that the particle size of the BFO synthesized at 500 °C is also less than 62 nm, which results in the weak ferromagnetic property, originating from canting of spin arrangement and the suppression of spiral spin arrangement [16].

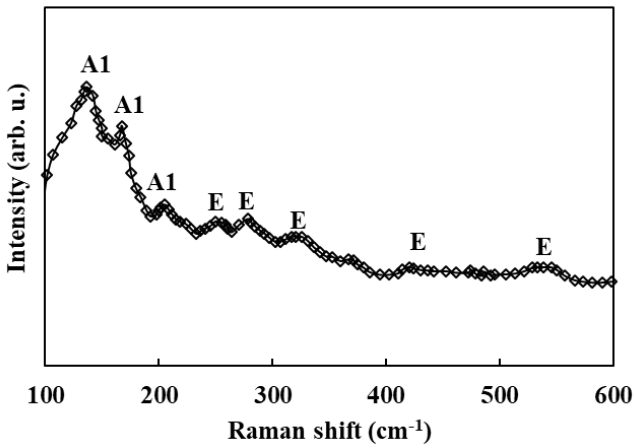

Fig. 3. Raman spectrum of BFO nanoparticles synthesized at 600 °C.

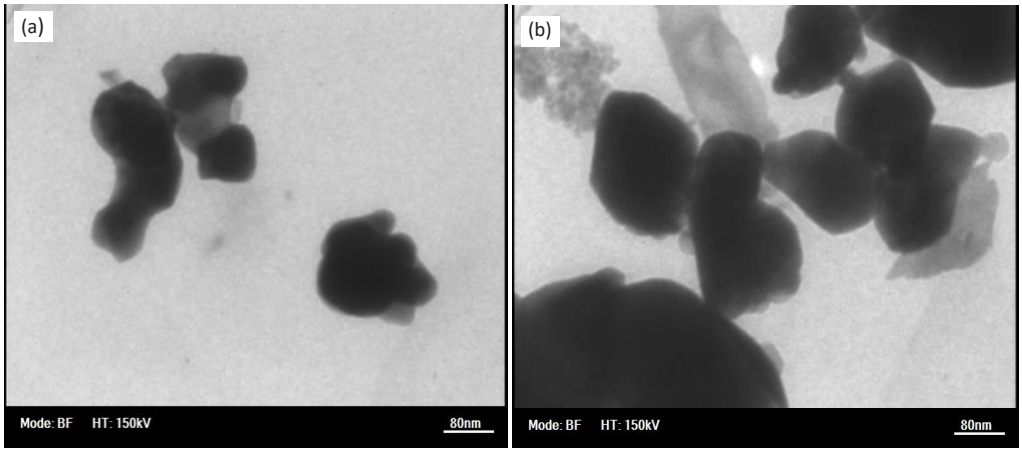

Fig. 4. TEM images of $BiFeO_3$ nanoparticles synthesized at (a) 500 °C and (b) 600 °C.

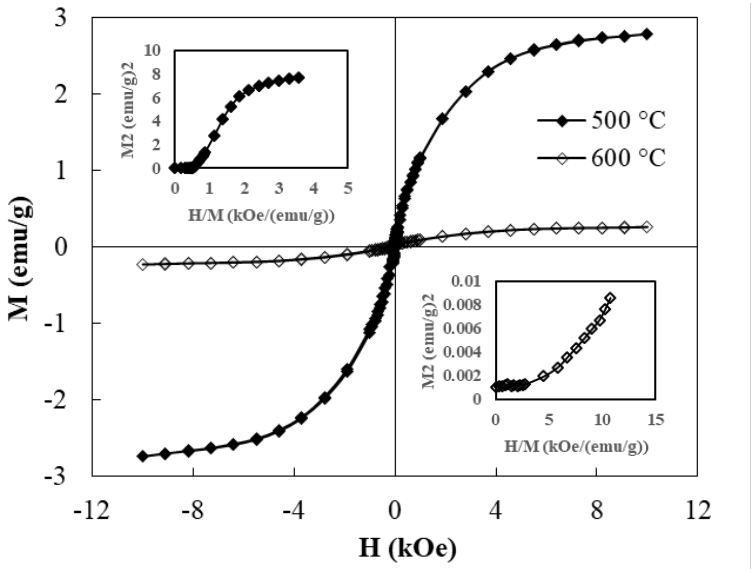

Fig. 5. Magnetization of the BFO nanoparticles synthesized at 500 and 600 °C (Inset shows ABK plot)

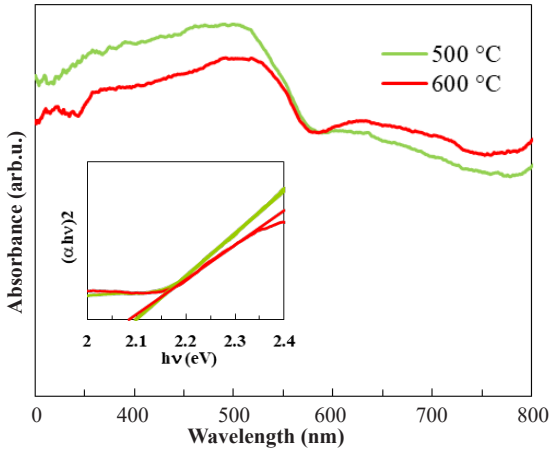

Fig. 6. UV−Vis absorption spectra and Tauc's plots ($(\alpha h\nu)^2$ vs. hν) of $BiFeO_3$ nanoparticles.

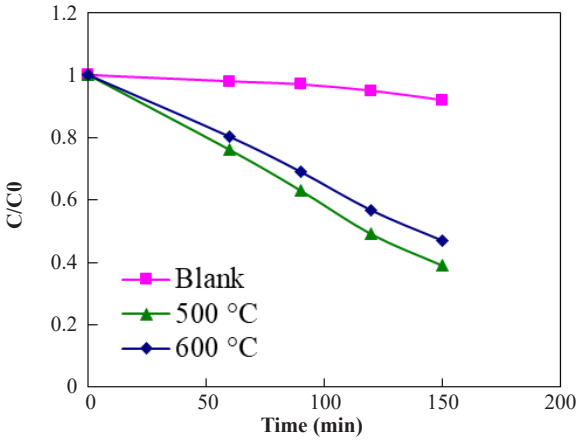

Fig. 7. Photodegradation of MB under sunlight irradiation by the BFO nanoparticles synthesized at 500 and 600 °C.

The ferromagnetic behavior can be confirmed by the convex shape of the Arrott–Belov–Kouvel (ABK) plot ABK plot [17], as shown in the inset of Fig. 5. However, the concave nature of the BFO synthesized at 600 °C in ABK plot denotes the presence of antiferromagnetic nature, due to the larger particle than 62 nm.

The UV−vis absorption spectra of the BFO nanoparticles are depicted in Fig. 6. The absorption spectra show that the $BiFeO_3$ nanoparticles can absorb considerable amounts of visible light, suggesting their potential applications as visible-light photocatalysts. The optical direct band gap, Eg, can be determined by the equation $(ahv)^2=A(hv-Eg)$, where hv is the photon energy in eV, α is the absorption coefficient, and A is a material dependent constant [13]. The measured band gap of $BiFeO_3$ synthesized at 500 and 600 °C is 2.10 and 2.08 eV, respectively. The band gap energy slightly increases with decreasing of the thermal decomposition temperature due to the drop in crystallite size (from 52 to 35 nm) according to the quantum-size effect [13].

The photodegradation results of MB dye by BFO nanoparticles are shown in the Fig. 7. In the absence of the BFO particles, the self-degradation of MB under the visible light irradiation was insignificant. In the presence of the BFO nanoparticles, the visible light irradiation for 90 min resulted in the 61% and 53% degradation of MB for the samples synthesized at 500 and 600 °C, respectively. Generally, the excellent photocatalytic activity of a semiconductor was related to (a) the fast transporting rate of charge carrier and the slow recombination rate of the photon-induced e^-/h^+, and (b) more surface

sites for adsorbing the reactants and leading to photodecompose the pollutants [18]. With the particle size decreasing through decreasing thermal decomposition temperature, the number of surface active catalytic-sites increases, so does the charge transfer rate during the photocatalysis [19].

CONCLUSIONS

The structure, magnetic properties and optical properties of the BFO nanoparticles synthesized by thermal decomposition of the glyoxylate precursor were studied. The BFO nanoparticles exhibit the ferromagnetic nature for thermal decomposition at 500 °C, while the antiferromagnetic behavior prevail at 600 °C, due to the large particle size. Furthermore, the photodegradation of MB dyes under sunlight irradiation by the synthesized BFO nanoparticles was investigated. The results indicated that the photocatalytic efficiency of BFO nanoparticles increased with the decreasing of particle size through controlling of decomposition temperature.

CONFLICT OF INTEREST

The authors declare that there are no conflicts of interest regarding the publication of this manuscript.

REFERENCES

1. Jiang L.M, Zhou G, "Facile synthesis of monodispersed nanocrystalline anatase TiO_2 particles with large surface area and enhanced photocatalytic activity for degradation of organic contaminant in wastewaters", Mat. Sci. Semicon. Proc., 2012; 15:108–111.
2. Gole J. L, Stout J. D, Burda C, Lou Y. B, Chen X.B, "Highly Efficient Formation of Visible Light Tunable $TiO_{2-x}Nx$ Photocatalysts and Their Transformation at the Nanoscale", J. Phys. Chem. B, 2004; 108:1230–1240
3. Gong L, Zhou Z, Wang S, Wang B, "Preparation and characterization of $BiFeO_3$@Ce-doped TiO_2 core-shell structured nanocomposites", Mat. Sci. Semicon. Proc., 2013; 16:288-294.
4. Soltani T, Entezar M. H, "Photolysis and photocatalysis of methylene blue by ferrite bismuth nanoparticles under sunlight irradiation", J. Mol. Catal. A: Chem., 2013; 377:197–203.
5. Kakuta N, White J.M, et al., "Surface analysis of semiconductor-incorporated polymer systems. 1. Nafion and cadmium sulfide-Nafion", J. Phys. Chem., 1985; 89: 48–52.
6. Reddy V. A, Pathak N. P, Nath R, "Particle size dependent magnetic properties and phase transitions in multiferroic $BiFeO_3$ nano-particles", J. Alloys Compd., 2012; 543: 206–212.
7. Hou Z. L, Zhou H. F, Yuan J, Kang, Yang H. J, Jin H. B, Cao M. S, "Enhanced Ferromagnetism and Microwave Dielectric Properties of $Bi_{0.95}Y_{0.05}FeO_3$ Nanocrystals", Chin. Phys. Lett., 2011; 28:037702.
8. Shami M. Y, Awan M. S, Rehman M. A, "Phase pure synthesis of $BiFeO_3$ nanopowders using diverse precursor via co-precipitation method", J. Alloys Compd., 2011; 509:10139–10144
9. Xu J. H, Ke H, Jia D. C, Wang W, Zhou Y, "Low-temperature synthesis of $BiFeO_3$ nanopowders via a sol–gel method", J. Alloys Compd., 2009; 472:473–477
10. Das N., Majumdar R., Sen A., Maiti H.S, "Nanosized bismuth ferrite powder prepared through sonochemical and microemulsion techniques" Mater. Lett., 2007; 61:2100–2104.
11. Stefanescu M, Caizer C, Stoia M, Stefanescu O, "Ultrafine, perfectly spherical Ni–Zn ferrite nanoparticles, with ultranarrow distribution, isolated in a silica matrix, prepared by a novel synthesis method in the liquid phase", Acta Mater., 2006; 54:1249–1256.
12. Stefanescu O, Vlase T, Vlase G, Doca N, Stefanescu M, "Synthesis and characterization of new hydroxycarboxylate compounds obtained in the redox reaction between $Fe(NO_3)_3$ and diol", Therm. Acta., 2011; 519:22–27.
13. Wang H, Zheng Y, Cai M, Huang H, Chan H. W, "First-principles study on the electronic and optical properties of $BiFeO_3$", Solid State Commun., 2009; 149:641-644.
14. Chen P, Xu X, Koenigsmann C, Santulli A. C, Wong S. S, and Musfeldt J. L, "Size-Dependent Infrared Phonon Modes and Ferroelectric Phase Transition in $BiFeO_3$ Nanoparticles", Nano Lett., 2010; 10:4526–4532.
15. Bhushan B, Basumallic A, Bandopadhyay S.K, Vasanthacharya N.Y, Das D, "Effect of alkaline earth metal doping on thermal, optical, magnetic and dielectric properties of $BiFeO_3$ Nanoparticles", J. Phys. D: Appl. Phys., 2009; 42 :065004.
16. Zhou H.F, Hou Z.L, Kong L.B, Jin H.B, Cao M.S, Qi X, "Enhanced magnetization and improved leakage in Er-doped BiFeO3 nanoparticles" Phys. Status Solidi A., 2013; 210: 809–813.
17. Nath T. K, Dutta P, and Dey P, "Magnetoimpedance, magnetoresistance, and magnetic properties of nanometric CMR manganites", J. Appl. Phys., 2008; 103:07F725
18. Vanga P. R, Mangalaraja R.V, Ashok M, "Structural, magnetic and photocatalytic properties of La and alkaline co-doped $BiFeO_3$ nanoparticles", Mater. Sci. Semicond. Process., 2015; 40:796–802
19. Hao C, Wen F, "Photocatalytic performances of $BiFeO_3$ particles with the average size in nanometer, submicrometer, and micrometer", Mater. Res. Bull., 2014; 50:369–373.